

# Application of Quality by Design principles in the development and evaluation of semisolid drug carrier systems for the transdermal delivery of lidocaine

Mónika Bakonyi<sup>a</sup>, Szilvia Berkó<sup>a</sup>, Anita Kovács<sup>a</sup>, Mária Budai-Szűcs<sup>a</sup>, Nikolett Kis<sup>a</sup>, Gábor Erős<sup>b,c</sup>,  
Ildikó Csóka<sup>a</sup>, Erzsébet Csányi<sup>a,\*</sup>

<sup>a</sup> Institute of Pharmaceutical Technology and Regulatory Affairs, University of Szeged, Szeged, H-6720, Hungary

<sup>b</sup> Department of Dermatology and Allergology, University of Szeged, Szeged, H-6720, Hungary

<sup>c</sup> Department of Oral Biology and Experimental Dental Research, University of Szeged, Szeged, H-6720, Hungary

\*: Corresponding author at: Institute of Pharmaceutical Technology and Regulatory Affairs, University of Szeged, H-6720, Eötvös u. 6, Hungary.

E-mail address: csanyi@pharm.u-szeged.hu (E. Csányi)

## 1. Abstract

The aim of this work was the formulation and comparison of different drug carrier systems for the transdermal delivery of lidocaine. Quality target product profile and quality attributes were identified, and an initial risk assessment was made according to the Quality by Design methodology. The critical quality attributes influencing the quality and efficacy of the final drug formulation were then defined in order to select the control points and proper methods for measurements. Four formulation types, each containing 5 % lidocaine were compared: conventional hydrogel, oleogel, lyotropic liquid crystal and nanostructured lipid carrier. Microscopic analysis, particle size and zeta potential measurements, Fourier transform infrared spectroscopy and Raman spectroscopy were performed to characterize the critical parameters in case of the different vehicles. Membrane diffusion and penetration studies were completed as well for each formulation *in vitro* and *ex vivo*, followed by measurements on skin hydration and transepidermal water loss *in vivo*. Our results lead us to the conclusion that the nanostructured lipid carrier is the most promising vehicle for the topical delivery of lidocaine. It showed the best penetration properties through heat separated epidermis and the highest moisturizing effect which are the most critical parameters based on the Quality by Design initial risk assessment and evaluation.

### Keywords:

Lidocaine

Topical anesthesia

Skin penetration

Nanostructured lipid carrier (NLC)

Lyotropic liquid crystal (LLC)

Quality by Design (QbD)

### Abbreviations:

CMA, Critical Material Attributes; Conc., Concentration; CPP, Critical Process Parameters; CQAs, Critical Quality Attributes; EMLA, Eutectic mixture of local anesthetics; FT-IR, Fourier transform infrared spectroscopy; IPM, Isopropyl myristate; LID, Lidocaine; LLC, Lyotropic liquid crystal; NLC, Nanostructured lipid carrier; PBS, Phosphate buffer saline; PS, Particle size; QbD, Quality by Design; QTPP, Quality Target Product Profile; REM, Risk Estimation Matrix; TEWL, Transepidermal water loss; TPP, Target Product Profile; ZP, Zeta potential.

## 2. Introduction

Semisolid systems are the most usual formulations for the delivery of drugs through the skin. Topically applied anesthetics are employed in order to eliminate the pain caused by needle insertion and injection, thus ameliorating patient compliance. Furthermore, they are devoid of the symptoms of superficial trauma and local reaction (i.e. erythema, venous sequelae, nerve damage) [1].

However, most of the marketed topical formulations have moderate skin penetration properties, rapid but short effect, thus the development of local topical anesthetics with a release in a prolonged fashion at the site of action is desperately desired [2]. Therefore, this work was undertaken to develop and compare a new formulation of lidocaine (LID), proposed to improve its clinical effectiveness in topical anesthesia in terms of both enhanced anesthesia and a prolonged duration of action.

For the goal that has been set, the penetration of lidocaine into the dermal layer is required. The sustained release of the drug is desired in order to improve patient compliance during long term treatments [3]. To satisfy the requirements of industrial and regulatory aspects, long term stability and appropriate dosage strength are also essential.

For this purpose, we investigated new topical drug delivery systems, such as lyotropic liquid crystals (LLC) and nanostructured lipid carriers (NLC), which can provide the above-mentioned increased duration of local action [4]. We incorporated LID as a free base into oleogel, LLC and NLC, and compared it with the LID hydrochloride containing hydrogel as a control. Hydrogel and oleogel are conventional drug carrier systems with a simpler structure than NLC and LLC. The marketed formulations contain LID hydrochloride in various concentrations (1-5 %, w/w) incorporated in ointment, gel, and solution [5]. The ionized form of LID can penetrate more rapidly than the free base but it is quickly absorbed and cleared off by the cutaneous capillaries [6].

LLC systems are becoming increasingly widespread because of their ability to be excellent drug carriers since they have a unique, skin-similarly structure and attractive physicochemical properties as they show a structure typical of fluids and the crystalline state of solids as well. They form gel-like phases with special internal structures, into which drugs can be loaded [7]. Their preparation is cost effective and easy as they are usually formed with low energy input from water and one or two surfactants and possibly cosurfactants in the definitive amounts of the components. Further advantages of these systems include easy storage, thermodynamic stability, sustained drug release, and similarity to colloid systems in living organisms. LLC systems with a lamellar structure demonstrate the greatest similarity to the intercellular lipid membrane of the skin, so they are primarily recommended for the development of a dermal dosage form [8].

Drug release from lyotropic liquid crystals depends on the percent ratio of water or water-surfactant in the lamellar liquid crystals, the presence of the totally lipophilic components, and the dissociation of the drug. A previous study revealed that the lidocaine base is able to diffuse freely through the liquid crystalline system, while the diffusion of the hydrochloride salt is delayed because this form is entrapped within the water layers of the lamellae [9].

New approaches in topical local anesthetic treatments include the use of the eutectic mixture of the local anesthetics (EMLA) lidocaine and prilocaine and the application of liposomal lidocaine, which has several advantages, like a faster onset of action and fewer adverse effects. This liposomal formulation is available under the trade names Maxilene 4 (RGR Pharma, Windsor, Ontario) and LMX (formerly ELA-Max; Ferndale Laboratories, Ferndale, Michigan) [10].

It has been shown that the incorporation of lidocaine into liposomes results in higher effectiveness, making shorter application periods as well as a decrease in side effects possible [6]. However, NLCs are modern alternatives of liposomes with many advantages, such as better physical stability, low cost (no need of expensive phospholipids), possibility of scale-up and manufacturing, potential in epidermal targeting, follicular delivery, controlled drug delivery and photostability improvement of active pharmaceutical ingredients [5].

NLCs are the second generation of lipid nanoparticles wherein solid lipid is partially substituted by liquid lipids. This structure allows the drug to be located in the liquid lipid, which predicts the better mobility of the drug, therefore improved stability and controlled drug release [11]. Additionally, the similarity of NLC forming lipids to physiological molecules makes these systems well tolerated, biodegradable and non-toxic. The interaction of the lipid nanoparticles with the skin lipids and sebum is dependent on the hydrophobicity of the incorporated molecule, the location of the drug within the formulation (incorporated into a lipid matrix or on the surface) and the type of the interacting skin lipid [12]. Furthermore, lipid particles, when the particle size is less than 200 nm, form a thin layer on the skin surface, reducing the transepidermal water loss and increasing the hydration, thereby they facilitate the penetration of the incorporated drug and support the physiological conditions of the skin [13–16]. Previous work proved that lidocaine NLC formulation can provide 2.5 h deep local anesthesia, and the total duration of anesthesia was up to 6 h, while the application of the conventional gel provided only 1 h of total anesthesia [5]. Other *in vitro* release studies showed reduced permeation through the skin, which could be related to a high reservoir capacity of the stratum corneum, due to the interaction between the lipid components of NLCs and the SC lipid matrix [17–20]. To develop formulations suitable for dermal application, NLC was incorporated in a hydrogel-based system.

Quality by Design (QbD) in pharmaceuticals is a systematic, scientific, risk-based, holistic and proactive method that begins with determining objectives and puts emphasis on understanding product and processes control [21–23]. In the development of new pharmaceutical formulations, the application of QbD approach results in a fast and improved optimization process by determining the quality target product profile (QTPP) and the critical quality attributes (CQAs) [24–27] Risk assessment is carried out to identify the potential hazards and parameters which possibly affect product quality [28]. We applied some initial elements of this method to effectively choose the best formulation regarding the target of this work (Figure 1).

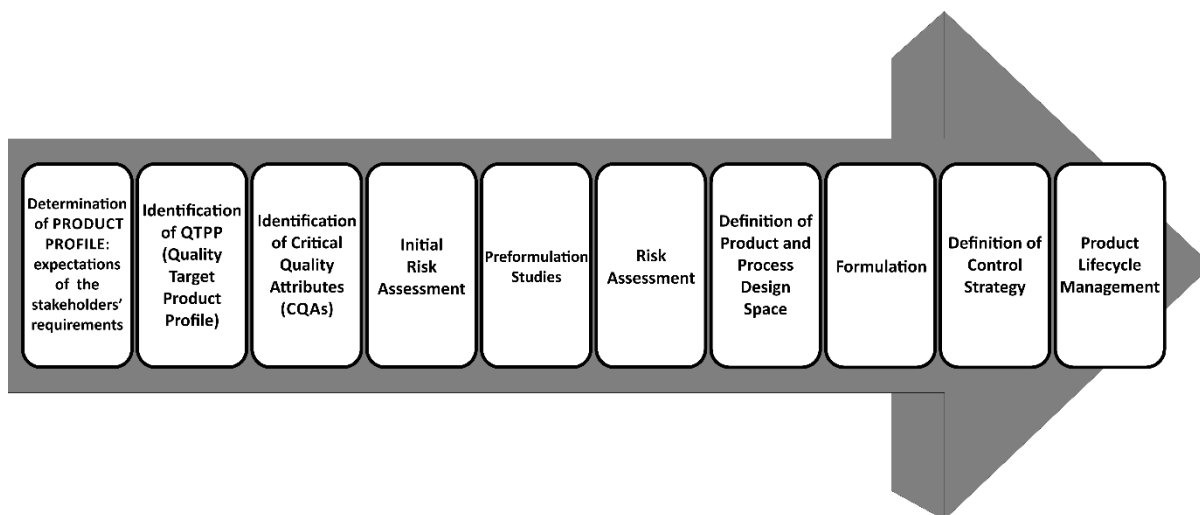


Fig 1. Flow chart of Quality by Design approach in formulation development.

### 3. Materials and methods

#### 3.1 Materials

Lidocaine, Lidocaine hydrochloride and Macrogol 400 were obtained from Hungaropharma Ltd. (Budapest, Hungary). Aerosil® 200 was purchased from Sigma-Aldrich (Budapest, Hungary). Cremophor® RH 40 (PEG-40 Hydrogenated Castor Oil; HLB value: 14–16) and Cremophor® RH 60 (PEG-60 Hydrogenated Castor Oil; HLB value: 15–17) were kindly supplied by BASF SE Chemtrade GmbH (Ludwigshafen, Germany). Miglyol® 812 N (caprylic/capric triglyceride) was a gift by Sasol GmbH (Hamburg, Germany). Isopropyl myristate (IPM) was purchased from Merck Kft. (Budapest, Hungary), Methocel™ K4M (hydroxypropyl methylcellulose) was from Colorcon (Budapest, Hungary) and Apifil® (PEG-8 Beeswax) was a gift from Gattefossé (St. Priest, France). The water used was purified and deionized with the Milli-Q system (Millipore, Milford, MA, USA).

#### 3.2 Quality by design methodology

##### 3.2.1 Definition of the QTPP and CQAs

The first step of the product development based on the QbD approach is the definition of the target product profile (TPP), which includes the definition of the dosage form, route of administration, dosage strength, etc. QTPPs are determined to ensure the quality, safety and efficacy of the product, and general elements of a QTPP for a dermal formulation are: site of activity, dosage form, release profile, etc. depending on the therapeutic aim.

The second step is to define the quality attributes of the formulation, namely to determine physicochemical and biological properties or characteristics that should be within the defined limit or distribution to ensure the desired product quality. These attributes determine the performance of the formulation, they are originated from the QTPP and they take prior knowledge as a basis. The CQAs are usually defined properties, like physical attributes, viscosity, homogeneity of the semisolid dosage form [29].

##### 3.2.2 Initial risk assessment: risk analysis of CQAs

A combination of the probability of occurrence of risk and severity of the risk is defined as risk assessment according to ICH Q9 quality risk management [28]. Performing this step before the development of a product can help the researcher to decide which studies need to be conducted. With the help of this method, critical and non-critical variables can be defined to establish a control strategy for in process and final testing. We evaluated the risks using an Ishikawa diagram. The risk estimation matrix (REM) presents the interdependence rating between QTPPs and CQAs. Based on the REM data, a Pareto chart can be designed, which shows the greatest chance of affecting the final quality of the product, and can be employed to assign the critical attributes which should be investigated during the development process. The screening of the parameters and the definition of the critical control points were carried out by the LeanQbD™ software (QbD Works LLC, Fremont, CA, USA). The Ishikawa diagram was constructed to identify the effect of key material attributes and process parameters for the optimized development of semisolid systems (Figure 2).

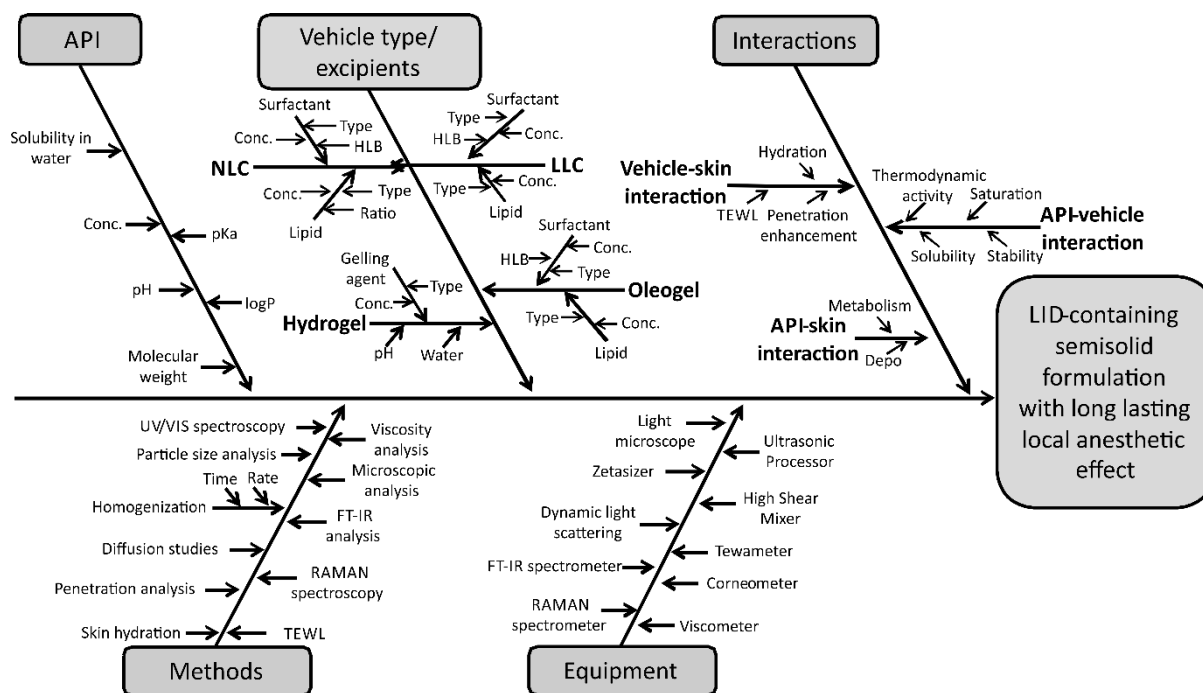


**Fig. 2.** Ishikawa diagram  
**Notes:** Conc. refers to “concentration”

### 3.3 Sample preparation

#### 3.3.1 Conventional hydrogel

The conventional hydrogel was prepared from 5 % (w/w) lidocaine hydrochloride dissolved in the mixture of purified water, ethanol and macrogol 400, and 3 % (w/w) Methocel K4M was added to this solution as the gelling agent.

#### 3.3.2 Oleogel

To formulate the oleogel, Mygliol 812 N and Cremophor® RH 40 (as a penetration enhancer) mixture was heated (60 °C) and 5 % (w/w) lidocaine base was dissolved in this mixture. 5 % (w/w) Aerosil 200 was added to prepare gels.

#### 3.3.3 Lyotropic liquid crystal

Samples produced with oil-surfactant (IPM: Cremophor® RH40= 1:4) mixture were heated (60 °C) and homogenized with a magnetic stirrer, 5 % (w/w) lidocaine base was dissolved and 10 % (w/w) of water was then added to the lipid phase in small amounts under stirring.

#### 3.3.4 Nanostructured lipid carrier

The solid lipid was melted at 80 °C, and Mygliol 812 N and lidocaine were added under moderate stirring. Under the same conditions, the water phase was prepared with surfactant (Cremophor® RH60) and HPLC water. Then the water phase was added to the lipid phase and put under high shear homogenizer for 1 minute (8000 rpm). The obtained pre-emulsion was ultrasonified using a Hielscher UP200S compact ultrasonic homogenizer (Hielscher Ultrasonics GmbH, Germany) for one cycle, 70 % amplitude, 10 min. In the end, the sample was cooled down in ice bath to get the NLC dispersion. Then, a gel was formed (at room temperature) with glycerin and Methocel K4M and the NLC dispersion was added to reach a final 5 % (w/w) lidocaine concentration.

### 3.4 Characterization of the carrier systems

#### 3.4.1 Microscopic analysis of LLC

The LLC samples were investigated under polarized light microscopy in order to study the texture of the lamellar phases. A small quantity of the sample was placed on a clean glass slide and observed under crossed polars using a magnification of 200×.

#### 3.4.2 Particle size and zeta potential of NLC

The average particle size (PS, z-average size) and zeta potential (ZP) of the NLC formulation were determined by dynamic light scattering with a Zetasizer Nano ZS device (Malvern Instruments, UK). The measurement medium was purified water with a refractive index of 1.33. The sample was thermostated to 25 °C and

measurements were made in disposable folded capillary cells. Each measurement was done in triplicate. To calculate the ZP from the electrophoretic mobility, the Helmholtz-Smoluchowski equation was applied.

Zeta potential below  $30\text{ mV}$  is considered to be stable, but many studies demonstrated that not only electrostatic repulsion influences the stability of nanoparticles but the use of a steric stabilizer (like Cremophor® RH 60 in this formulation) also supports the formation of a stable nanoparticle dispersion [30].

### 3.4.3 Fourier transform infrared spectroscopy analysis of NLC

The Fourier transform infrared spectroscopy (FT-IR) spectra of the NLC were recorded with an Avatar 330 FT-IR spectrometer (Thermo Fisher Scientific Inc., Waltham, MA, USA) equipped with a horizontal ATR crystal (ZnSe,  $45^\circ$ ), between  $4000$  and  $400\text{ cm}^{-1}$ , with 128 scan, at an optical resolution of  $4\text{ cm}^{-1}$ . For the spectral analysis Thermo Scientific GRAMS/AI Suite software (Thermo Fisher Scientific Inc., Waltham, MA, USA) was used.

### 3.4.4 Raman spectroscopy measurements of NLC

The Raman spectra of the NLC was acquired with a Thermo Fisher DXR Dispersive Raman Spectrometer (Thermo Fisher Scientific Inc., Waltham, MA, USA) equipped with a CCD camera and a diode laser operating at  $532\text{ nm}$ . The spectra of the NLC components, lidocaine-free and LID-NLC samples were with an exposure time of  $6\text{ s}$ , with 24 scans, including cosmic ray and fluorescence corrections. Measurements were carried out with a laser power of  $10\text{ mW}$  at a slit width of  $25\text{ }\mu\text{m}$ .

## 3.5 Drug diffusion and penetration investigations

### 3.5.1 Preparation of heat-separated epidermis

Excised human skin was obtained from a Caucasian female patient who underwent abdominal plastic surgery, with the approval of the Ethical Committee of the University of Szeged, Albert Szent-Györgyi Clinical Centre (Human Investigation Review Board license number: 83/2008.). For the separation of epidermis, the heat separation technique was applied [31]. The obtained epidermal membrane was applied onto the surface of PBS (phosphate buffer solution,  $\text{pH} = 7.4$ ) for at least  $20\text{ min}$  and then set on a supporting mixed cellulose ester membrane (Porafil, Machenerey-Nagel, Düren, Germany, and Pall Life Sciences, Washington, NY, USA; pore diameter  $0.45\text{ }\mu\text{m}$ ) for the measurements.

### 3.5.2 Franz diffusion cell method

*In vitro* and *ex vivo* permeation of LID was measured using a vertical Franz diffusion cell system (Hanson Research, Chatsworth, CA, USA) in a six-unit assembly (effective permeation area  $1.676\text{ cm}^2$ ) for  $24\text{ h}$  at  $37\pm 0.5\text{ }^\circ\text{C}$ . The donor phase was  $0.30\text{--}0.40\text{ g}$  of the appropriate formulation, which was placed on a mixed cellulose ester membrane (Porafil, Machenerey-Nagel, Düren, Germany, and Pall Life Sciences, Washington, NY, USA) itself (*in vitro*), or in the case of *ex vivo* measurements the epidermis was supported with a Porafil membrane filter. Phosphate buffer saline (PBS)  $\text{pH} 7.4$  was used as the acceptor medium and it was stirred at  $450\text{ rpm}$  throughout the experiment. At selected time intervals, samples of  $0.8\text{ mL}$  were taken from the acceptor phase by the autosampler (Hanson Research, Chatsworth, CA, USA) and replaced with an equal volume of fresh receiver medium. The amount of permeated drug was measured using a Unicam Helios Thermospectronic UV-VIS spectrophotometer (Unicam, Thermo Fisher Scientific Inc., Waltham, MA, USA) at  $262\text{ nm}$ . Five parallel measurements were carried out and the amount of LID penetrating during a time period was plotted. The results were expressed as means  $\pm$  SD for the evaluation of drug release kinetics.

### 3.5.3 Penetration analysis

The *in vitro* and *ex vivo* penetration of LID was calculated in terms of the mean cumulative amount permeated through the membrane, taking the diffusion area into account. The results were plotted as a function of time. The steady state flux ( $J$ ) was calculated from the slope of the linear regression versus  $t^{1/2}$  and expressed in  $\mu\text{g cm}^{-2}\text{ h}^{-1}$ .

## 3.6 Measurement of skin hydration and transepidermal water loss

3-4-month-old male SKH-1 hairless mice were employed to evaluate the effect of LID-free formulations on skin hydration and transepidermal water loss. The mice were kept in a thermoneutral environment with a 12 h light-dark cycle in plastic cages and they had access to standard laboratory chow and water ad libitum. All experiments were in full accordance with the NIH guidelines and the interventions were approved by the Ethical Committee for the Protection of Animals in Scientific Research at the University of Szeged (license number: V./145/2013). Prior to the treatments, the animals were anesthetized with a mixture of ketamine ( $90\text{ mg/kg}$  bodyweight) and xylazine ( $25\text{ mg/kg}$  bodyweight), administered intraperitoneally. At the end of the experiments, the mice were euthanized with an overdose of ketamine ( $300\text{ mg/kg}$ ).

For the treatment,  $0.2\text{ g}$  of each formulation was deposited on the dorsal skin surface of hairless mice, left for  $30\text{ minutes}$  for penetration, and after the diffusion period the skin surface was cleaned with a dry cotton swab.

Skin hydration was measured using a Corneometer CM 825 (Courage und Khazaka, Germany) and TEWL was evaluated with Tewameter TM 300, both connected to a Multi Probe Adapter MPA 5 (Courage und Khazaka,

Germany), 30, 90 and 150 minutes after the application. The results are given in percentage compared to the levels before treatment.

### 3.7 Statistical analysis

The results were analysed statistically with the two-way ANOVA analysis of variance (Bonferroni post-test) using Prism for Windows software (GraphPad Software Inc., La Jolla, CA, USA). Differences were regarded as significant if  $p < 0.05^*$ ,  $p < 0.01^{**}$  and  $p < 0.001^{***}$  versus the control.

## 4. Results and discussion

### 4.1 Definition of QTPP and CQAs

We aimed to develop a semisolid local anesthetic formulation for dermal use, which can provide effective and prolonged anesthesia. This therapeutic efficacy of the formulations depends on therapeutic indication, route of administration, site of activity, dosage form, release profile, stability and dosage strength. The CQAs are derived from the QTPPs. The quality attributes are identified as physical attributes, solubility of API in drug product, homogeneity of API in drug product, *in vitro* drug release, *ex vivo* drug release, moisturizing effect, TEWL, dosage form type and viscosity. Table 1 presents the list of QTPP and CQA parameters with their targets and justifications.

**Table 1**  
QTPP and CQAs of the target local anesthetic formulation

QTPP parameters	Target	Justification
Therapeutic indication	local anesthetic	Local anesthesia and pain alleviating are required in various minor surface-skin surgical conditions and invasive procedures. Local anesthetics are also available to provide temporary relief from pain, irritation and itching caused by various conditions.
Route of administration	Dermal	The dermal delivery of drugs is an opportunity to avoid systemic side effects and the hepatic metabolism of drugs, thus the application of lower doses is available. Furthermore, it is a non-invasive, easy-to-use method resulting in high patient compliance.
Site of activity	Topical	The topical activity of local anesthetic drugs is desired because of their systematic side effects. Topical formulations are designed to allow the dermal penetration of their actives into the deeper regions of the skin, such as the viable epidermis and the dermis, where the nerve fibers are located. The absorption into the systemic circulation is not the aim of these formulations.
Dosage form	Semisolid system	Semisolid systems offer many advantages, like easy application and pleasing rheological behavior, which enable them to adhere to the application surface and they are able to topically deliver many drug molecules.
Release profile	Sustained drug release	Prolonged duration local anesthesia is desirable to effectively treat pain and to reduce the number of applications, thus improving patient compliance.
Stability (physical, chemical, biological)	no visible sign of instability at the time of preparation and after 1 months (at room temperature)	It is essential to maintain the physical, chemical and biological stability of the product over time because stability issues, like phase separation, change in pH, viscosity, appearance and crystal formation can affect the release and therapeutic effect of the formulation.
Dosage strength	5g/100g	5% lidocaine formulations are effective as local, topical anesthetic preparations.
CQA	Target	Justification
Physical attributes (color, odor, appearance)	Clear, translucent or opaque appearance, and odorless smell	Physical attributes are not critical, but satisfactory appearance can improve patient compliance. However, they are not directly in connection with safety and efficiency.
Solubility of API in drug product	High (>90 %)	Drug solubility provides uniformity of dosage form by preventing phase separation. Furthermore, a high concentration gradient can increase the diffusion force across the skin.

Homogeneity of API in drug product	Homogenous distribution of the API	Homogeneity is crucial to provide the uniformity of dosage units during the application period.
<i>In vitro</i> drug release	Sustained (compared to control)	Slow drug release is required to provide prolonged anesthesia.
<i>Ex vivo</i> drug release	Sustained (compared to control)	Slow drug release is required to provide prolonged anesthesia. Permeability is less through human skin than synthetic membrane based on preliminary results in the literature.
Moisturizing effect	Increase of basal skin hydration (compared to control)	An increase of the water content of the skin promotes drug permeation.
TEWL	Minor and transient change in TEWL values (compared to control)	A high value of transepidermal water loss is related to the disruption of the barrier function of the skin.
Viscosity	Optimal spreadability of the product (range: 1000-50000 mPas)	Rheological properties, such as the viscosity of semisolid dosage forms, can influence their drug delivery. Viscosity may directly influence the diffusion rate of drug at the microstructural level.
Dosage form type	Penetration enhancing properties	The composition and the special structure of the vehicle can ameliorate the penetration of active agents.

## 4.2 Initial risk assessment

In this study, the initial risk assessment plan identified the critical quality attributes of product quality expectation. The risk estimation matrix presents the interdependence rating between the QAs and QTPPs on the three-level scale (Table 2). For the probability rating a 1 (low)-3 (medium)-9 (high) scale was used, considering all CQAs and their relationship to the QTTPs. The following properties were found to influence product quality: *in vitro* and *ex vivo* drug release (both 18 %), dosage form type (15 %), moisturizing effect and TEWL (both 13 %). Based on the REM results, a Pareto chart (Figure 3) was generated showing the severity scores of CQAs, which lead us to the following findings: *in vitro* and *ex vivo* drug release, dosage form type, moisturizing effect and TEWL with the highest severity score (>300), suggesting that these are the most critical characteristics influencing the quality of the formulation. The Pareto chart illustrates the critical attributes which have to be considered during the development process. Based on the results of the risk assessment, these points have been investigated in this research.

**Table 2**

Selected QTTPs and CMAs representing their interdependence rating with risk estimation matrix (Lean-QbD Software):  
Low = low risk parameter; Medium = medium risk parameter; High= high risk parameter.

QTTP		Dosage form (H)	Route of administration (H)	Site of activity (H)	Therapeutic indication (H)	Release profile (H)	Stability (M)	Dosage strength (M)
Physical attributes	2%	Low	Low	Low	Low	Low	Low	Low
Solubility of API	10%	High	Low	Low	Medium	High	Low	High
Homogeneity of API in drug product	7%	Medium	Low	Low	Medium	High	Medium	Medium
<i>In vitro</i> drug release	18%	High	High	High	High	High	Medium	High
<i>Ex vivo</i> drug release	18%	High	High	High	High	High	Medium	High
Moisturizing effect	13%	High	High	Medium	High	Medium	Low	Low
TEWL	13%	High	High	Medium	High	Medium	Low	Low
Viscosity	4%	Medium	Low	Low	Low	Medium	Medium	Low
Dosage form type	15%	High	High	Medium	High	High	Medium	Medium

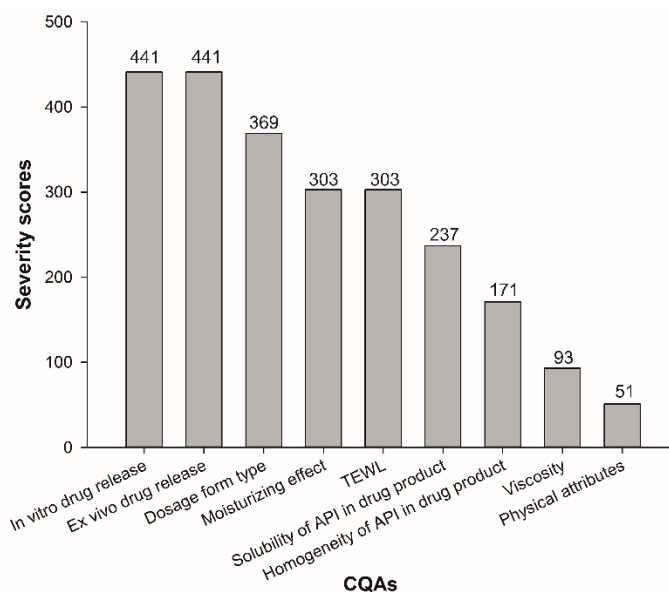


**Fig. 3.** Pareto analysis of the identified CQAs.

### 4.3 Polarization Microscopic Examinations

Figure 4 presents a polarized microscopic picture of the developed blank and lidocaine containing LLC structures, revealing a lamellar LLC pattern with a characteristic „Maltese cross” structure in polarized light [32]. Liquid crystals are anisotropic materials and they display characteristic textures between crossed polarizers under an optical microscope. These textures can be used to identify different liquid crystalline phases. Liquid crystals are visible by polarizing light microscopy as lipid circular droplets with characteristic birefringence in the shape of a Maltese cross. The presence of the Maltese cross indicates a parallel orientation of one of the main axes of the structure in the plane of polarization of the incident light, so linearly polarized light passing through will not change its polarization, resulting in dark regions [33].

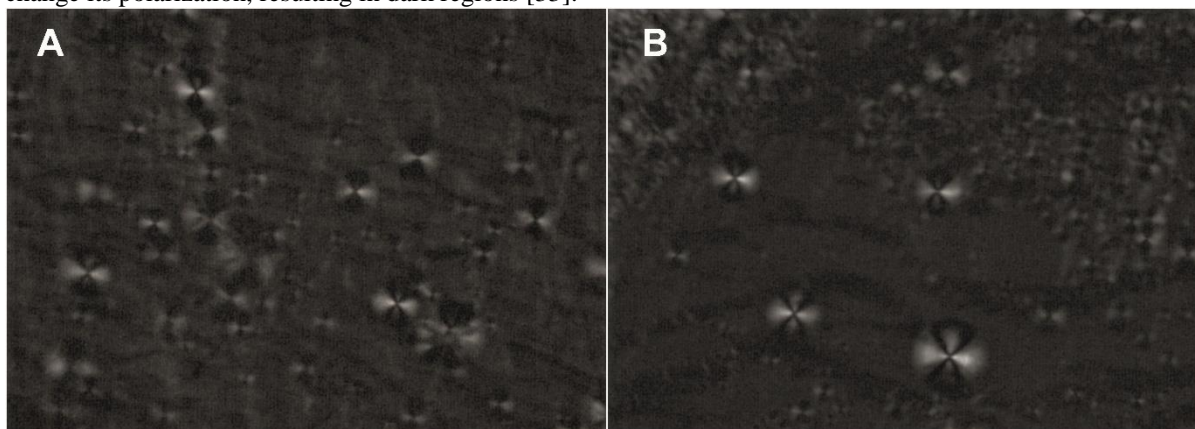


**Fig. 4.** Polarizing microscopic examination of blank (A) and lidocaine containing (B) LLC.

### 4.4 Results of particle size and zeta potential analysis

The particle size of the NLC system was  $87.61 \pm 0.55$  nm. The calculated polydispersity index was  $0.1615 \pm 0.01$ , referring to a monodisperse distribution [34,35]. The low polydispersity index predicts a satisfying stability of the system [13]. The zeta potential was  $-11.983 \pm 0.31$  mV.

### 4.5 FTIR and Raman analysis of NLC

For the determination of API-excipient interactions in the NLC formulation at the level of functional groups, we applied FT-IR and Raman spectroscopy. In order to evaluate chemical interaction among LID and the carriers, FT-IR and Raman spectra of Apifil®, Miglyol® 812 N, Cremophor® RH60, LID, LID-free NLC and LID-NLC formulations were studied as shown in Figure 5. The characteristic bands are presented in Table 3 with the vibrational assignments ( $\text{cm}^{-1}$ ) [36].



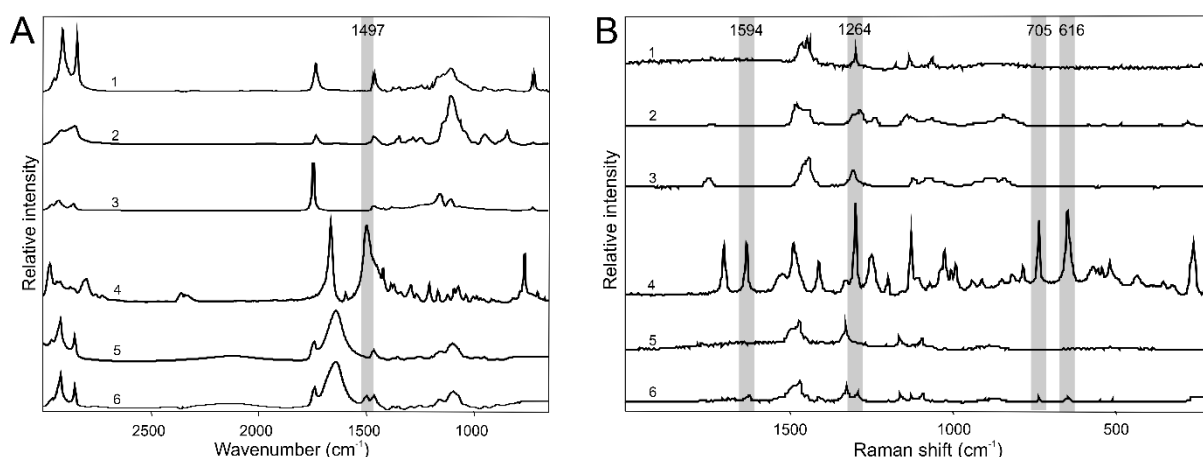


**Fig. 5.** FT-IR (A) and Raman (B) spectra of individual components and NLC compositions.

**Notes:** Apifil (1), Cremophor® RH60 (2), Mygliol 812 N (3), Lidocaine (4), Lidocaine-free NLC (5), Lidocaine NLC (6)

**Table 3**  
Observed FT-IR and Raman peaks (in  $\text{cm}^{-1}$ ) and peak assignments for lidocaine

Observed peaks <sup>a</sup>		Assignment
Infrared	Raman	
	3043 (m)	methyl antisymmetric stretching
2970 (s)	2973 (m)	methyl antisymmetric stretching
	2922 (vs)	CH <sub>2</sub> antisymmetric and symmetric stretching
2874 (s)	2875 (m)	methyl symmetric stretching
2800 (m)		CH <sub>2</sub> symmetric stretching
1664 (vs)	1664 (w)	C=O stretching
1593 (m)	1594 (vs)	HNC scissor deformation, NC amide stretching
1497 (vs)		methyl antisymmetric deformation
	1484 (m)	methyl antisymmetric deformation
	1452 (vs)	CH <sub>2</sub> scissor deformation
1421 (s)		methyl symmetric deformation
1385 (m)		CH <sub>2</sub> wag
	1375 (m)	CH <sub>2</sub> twist, CH <sub>2</sub> wag
1338 (w)		ring stretching deformation III, CH <sub>2</sub> twist, CH <sub>2</sub> wag
1292 (s)		CH <sub>2</sub> twist
	1264 (vs)	m-CH bend, o-CC symmetric stretching
1207 (s)	1215 (m)	amide NH stretching, CC stretching
1167 (s)	1164 (m)	NC <sub>2</sub> antisymmetric stretching, CH <sub>2</sub> rock, CH <sub>2</sub> twist
1121 (s)		m-CH bend, ring stretching deformation II
	1094 (s)	methyl rock, CH <sub>2</sub> twist
1074 (vs)	1075 (w)	methyl rock
1036 (s)	1037 (vw)	methyl rock
987 (m)	991 (m)	CH <sub>2</sub> rock, CH wag
	972 (w)	CH wag
	959 (w)	CC stretching, NCO scissor deformation
918 (w)	909 (vw)	CC stretching
	877 (w)	ring bend deformation, ring N-stretching
818 (m)		CH <sub>3</sub> rock
764 (vs)		CH wag
	754 (w)	ring torsional deformation, HNC wag
704 (s)	705 (vs)	HNC wag
	661 (m)	ring stretching deformation,
615 (s)	616 (vvs)	NCO wag
521 (m)	512 (vw)	ring torsional deformation II
488 (s)	486 (w)	ring bend deformation II
	232 (s)	o-CC wag

<sup>a</sup> Intensity abbreviations: vw: very weak, w: weak, m: medium, s: strong, vs: very strong, vvs: very very strong.

The intense band in the FT-IR spectrum of LID observed at 2970  $\text{cm}^{-1}$  is associated mostly with the methyl group antisymmetric stretching mode. The intense band at 1664  $\text{cm}^{-1}$  is assigned to C=O stretching band. The very strong intensity 1497  $\text{cm}^{-1}$  peak is composed mostly of mixed methyl and methylene deformations. A strong line is observed at 1296  $\text{cm}^{-1}$ , corresponding to the twisting of all methylene groups in the molecule. A group of strong and very strong intensity lines observed at 1207, 1167, 1121, 1074, and 1037  $\text{cm}^{-1}$  is calculated to have a high degree of mixing (N–C, C–C stretches, ring bending deformation I and II, N–C2 antisymmetric stretch, methylene rock and twist, methyl group rocking). The next lower group of intense bands in the IR spectrum begins with a very strong line at 764  $\text{cm}^{-1}$  and consists of CH wags and ring torsional deformation.

In the Raman spectra, LID exhibited characteristic peaks at 2922, 1594, 1452, 1264, 1094 and 705  $\text{cm}^{-1}$ . At 2922  $\text{cm}^{-1}$  there is a very intense line in the spectrum, which is calculated to be highly mixed from methylene  $\text{CH}_2$  stretching in the two ethyl groups. In the Raman spectrum the peak at 1594  $\text{cm}^{-1}$  corresponds to HNC scissoring and NC stretching modes. The peak at 1452  $\text{cm}^{-1}$  is mostly due to methylene scissoring. At 1263  $\text{cm}^{-1}$  a very intense line is observed, corresponding mainly to CH bending and C–C symmetric stretching modes. The strong peak at 1094  $\text{cm}^{-1}$  is attributed to methyl rock,  $\text{CH}_2$  twist and  $\text{NC}_2$  symmetric stretch. At about 705  $\text{cm}^{-1}$  there appears a very strong peak in the Raman spectrum consisting of HNC wag and twist and of ring torsional deformation.

The 1497  $\text{cm}^{-1}$  peak, related to the methyl functional groups of LID, is present in the FTIR spectra of LID-NLC, but absent from the spectra of the blank NLC, indicating the presence of LID in the lipid nanoparticle. As all the characteristic peaks of the drug and the excipients were present in the LID-NLC spectrum and no shifting of existing peaks or creation of new peaks were observable, this indicates that there were only physical interactions among the drug and the excipients, and no chemical interaction took place among them. The Raman measurements confirmed these results: the peaks at 616, 705, 1264, 1594  $\text{cm}^{-1}$ , which are the characteristic features of the LID spectra, are present in the LID-NLC spectra without shifting, and missing from the blank NLC. The absence of chemical interactions between the drug and the vehicle suggests that the release of lidocaine from the carrier system is not inhibited.

## 5. Result of in vitro release and ex vivo permeation studies

In Figure 6, the plots of the cumulative amounts of LID permeated through artificial mixed cellulose ester membrane (A) and human heat separated epidermis (B) as a function of time are shown. Drug flux values for formulations are reported in Table 4.

The *in vitro* diffusion of LID through the artificial membrane from the different formulations is illustrated in Figure 6A. The LLC formulation showed a complete release of LID at the end of 15-18 h. The conventional hydrogel exhibited a fast onset of permeation, but the permeation was not completed after 24 h (78.58 $\pm$ 2.50 %). The oleogel and NLC formulations provided a sustained release, 70.32 % $\pm$ 1.76% of the drug was released from the oleogel, 58.66 % $\pm$ 4.28 from NLC after 24 h.

*Ex vivo* penetration patterns were slightly different, presumably because of the interaction of the different vehicles and the skin lipids and proteins (Figure 6B). LID permeation from the oleogel exhibited the lowest value, only 9.84 $\pm$ 1.37 % of the drug penetrated after 24 h. There was no significant difference between the penetration of conventional hydrogel (15.05 % $\pm$ 3.70) and LLC (14.12 % $\pm$ 1.73) formulation. Surprisingly, through the epidermis, the NLC formulation exhibited the most complete penetration (19.44 % $\pm$ 5.05), whereas *in vitro* it was the lowest. This finding could be explained by the special structure of the NLC, which allows the high bioavailability of this formulation [2]. The components of the NLC formulation have similar lipophilicity as the skin, so they have good miscibility with the skin lipids, and this can cause greater penetration [37]. Our results are in good agreement with other studies, which revealed that lipid nanocarriers can improve penetration and effectiveness of encapsulated lidocaine [2,5,38,39]. The high penetration rate of LID through the epidermis predicts the fast accumulation of the drug in the dermis, which is the site of action for local anesthetics. Babaei et al. confirmed that NLC can penetrate through the epidermis and accumulate in the dermal layers of the skin [40]. The low permeation rates of oleogel could be explained by their composition: they do not contain any water (in contrast to the other formulations), so there will be no external supply of water, hydration can only be provided from the internal processes of the skin [41].

**Table 4**  
Steady-state fluxes of LID *in vitro* and *ex vivo* from different formulations

	Flux ( $\mu\text{g cm}^{-2} \text{h}^{-1}$ )	
	<i>in vitro</i>	<i>ex vivo</i>
Conventional hydrogel	2175.59	369.23
Oleogel	1844.57	259.66
LLC	3211.42	373.99
NLC	1682.02	618.05

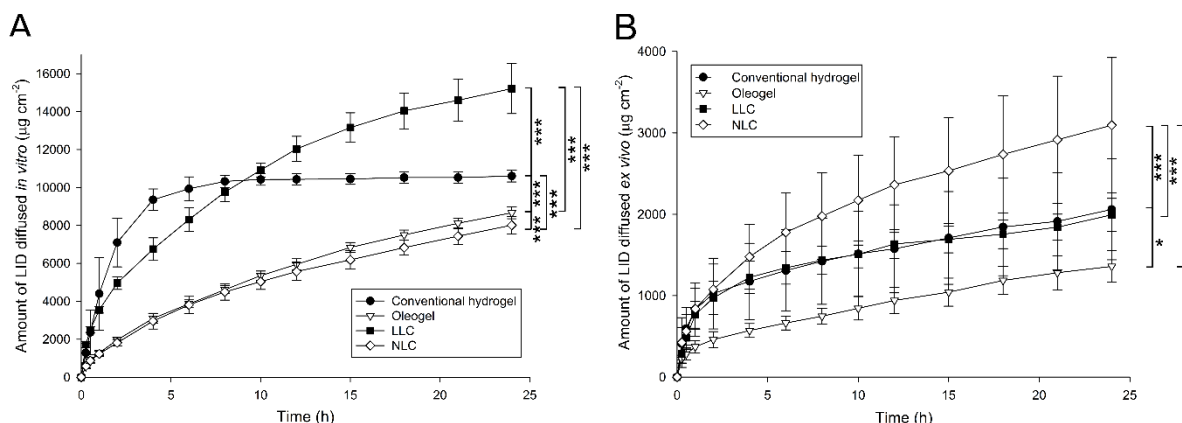


**Fig. 6.** *In vitro* (A) and *ex vivo* (B) diffusion studies of LID containing formulations.  $p < 0.05^*$ ,  $p < 0.01^{**}$  and  $p < 0.001^{***}$

## 6. Skin hydration and TEWL measurements

In skin hydration measurements (Figure 7A), there were no significant differences between the hydrating effect of conventional hydrogel and LLC. Both of them increased the hydration slightly after 30 minutes ( $13.63 \pm 5.23\%$  and  $18.42 \pm 3.12\%$ ), and this effect was shortened after 150 minutes ( $6.92 \pm 5.88\%$  and  $11.78 \pm 3.95\%$ ). However, oleogel caused a dramatic decrease of hydration after 30 minutes ( $-43.47 \pm 5.93\%$ ). This could be the result of the presence of Cremophor® RH40 in the formulation, which is a well-known penetration enhancer that disturbs the ordered lipid structure of the stratum corneum, resulting in the loss of water content [42]. Furthermore, in the oleogel formulation, there was no water as an excipient, so after the application there is no chance to supply the lost water from this source. After 150 minutes, the skin barrier seemed to have recovered partly, and the hydration value ( $-27.57 \pm 6.03\%$ ) was closer to the initial level. NLC resulted in a remarkable increase in skin hydration after 30 minutes ( $71.18 \pm 3.31\%$ ) and the hydration maintained a high level also after 150 minutes ( $64.65 \pm 5.46\%$ ).

The TEWL changes displayed notable differences between the effects of formulations (Figure 7B). NLC caused the slightest increase in TEWL ( $14.68 \pm 3.19\%$  after 30 minutes,  $18.46 \pm 2.45\%$  after 90 minutes and  $22.78 \pm 7.39\%$  after 150 minutes). It is well-known that lipid nanostructures with a particle size less than 200 nm form a lipid film on the skin surface, and owing to this occlusive effect, the TEWL changes will decrease, thus hydration will increase [43]. Our results confirmed these findings and are in good agreement with the *ex vivo* penetrations studies, because improved skin hydration and occlusion are shown to increase drug absorption from topical formulations [44].

Conventional hydrogel caused a slightly noticeable TEWL increase after 30 minutes ( $36.20 \pm 11.25\%$ ), but this effect was reduced after 150 minutes ( $19.71 \pm 5.71\%$ ). However, oleogel increased TEWL significantly ( $51.24 \pm 6.66\%$  after 30 minutes,  $67.33 \pm 9.06\%$  after 90 minutes and  $67.73 \pm 3.54\%$  after 150 minutes), which can explain the dramatic decrease in hydration values discussed earlier. The TEWL rise was the most significant for LLC. The increase was  $101.39 \pm 4.24\%$  after 30 minutes, and it still rose after 150 minutes to  $130.08 \pm 7.95\%$ . The reason for this huge water loss is definitely the high amount of surfactant (Cremophor® RH40) incorporated in the LLC formulation. However, skin hydration was not negatively affected because of the lamellar, water-containing structure of the LLC, which can provide excellent hydration and compensate for the high TEWL values [45].

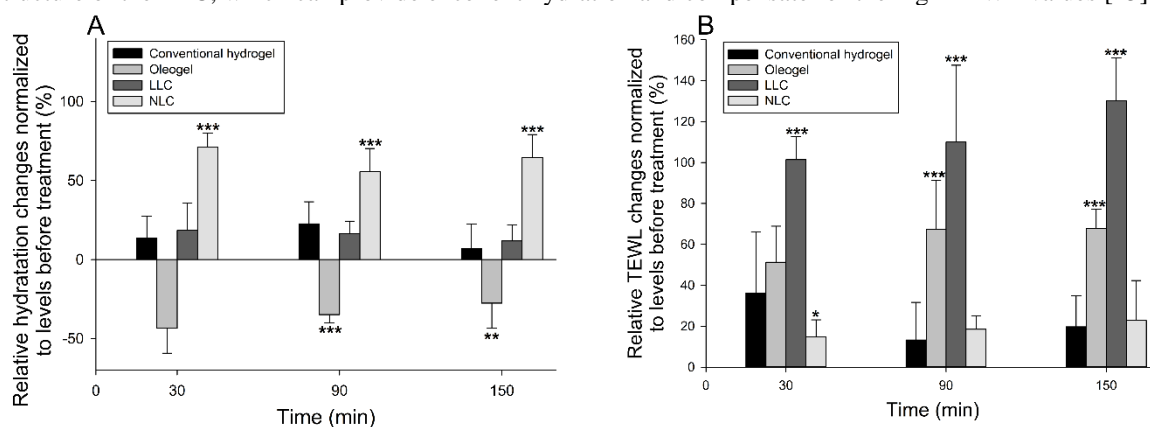


**Fig. 7.** Skin hydration (A) and transepidermal water loss (B) changes after exposure to formulations. Values are given as percentage referring to values before treatments vs. conventional hydrogel.  $p < 0.05^*$ ,  $p < 0.01^{**}$  and  $p < 0.001^{***}$


## 7. Conclusion

The selection of an adequate drug carrier system with proper material attributes for transdermal delivery is fundamental to reach the aim of application. In this work we compared the properties, skin penetration and hydrating effect of different formulations for the delivery of lidocaine by applying the QbD concept during the development process, which revealed the critical points that should be investigated.

The oleogel represented low penetration rates, both *in vitro* and *ex vivo*, and caused a negative effect on skin hydration. LLC showed a high release of the drug *in vitro*, and moderate flux values *ex vivo*, however, this formulation increased TEWL dramatically. The penetration of the NLC formulation was the most significant through heat separated epidermis after 24 hours, and the skin hydrating and occlusive effect makes it a favorable carrier system.

These findings suggest the use of novel nanostructured drug carrier systems for transdermal drug delivery, though further investigations are needed to completely understand the penetration profiles of these carrier systems, and to define the crucial factors affecting the drug release and diffusion. For the further development of the chosen system, critical material attributes (CMA) and critical process parameters (CPP) should be defined and comprehensive risk assessment steps are needed to be performed to understand the parameters that produce the final product with the required characteristics.

## Acknowledgements

 Supported BY the ÚNKP-16-3 New National Excellence Program of the Ministry of Human Capacities

**Declarations of interest:** none

## References

- [1] L.N. Ribeiro, M. Franz-Montan, M.C. Breitzkreitz, A.C. Alcantara, S.R. Castro, V.A. Guilherme, R.M. Barbosa, E. de Paula, Nanostructured lipid carriers as robust systems for topical lidocaine-prilocaine release in dentistry, *Eur J Pharm Sci.* 93 (2016) 192–202. doi:10.1016/j.ejps.2016.08.030.
- [2] C. Puglia, M.G. Sarpietro, F. Bonina, F. Castelli, M. Zammataro, S. Chiechio, Development, Characterization, and In Vitro and In Vivo Evaluation of Benzocaine- and Lidocaine-Loaded Nanostructured Lipid Carriers, *J. Pharm. Sci.* 100 (2011) 1892–1899. doi:10.1002/jps.22416.
- [3] A.J. Claxton, J. Cramer, C. Pierce, A systematic review of the associations between dose regimens and medication compliance, *Clin. Ther.* 23 (2001) 1296–1310. doi:10.1016/S0149-2918(01)80109-0.
- [4] G. Barratt, Colloidal drug carriers: achievements and perspectives, *Cell Mol Life Sci.* 60 (2003) 21–37. <http://www.ncbi.nlm.nih.gov/pubmed/12613656>.
- [5] P. Pathak, M. Nagarsenker, Formulation and evaluation of lidocaine lipid nanosystems for dermal delivery, *AAPS PharmSciTech.* 10 (2009) 985–992. doi:10.1208/s12249-009-9287-1.
- [6] M.S. Nagarsenker, A.A. Joshi, Preparation, characterization, and evaluation of liposomal dispersions of lidocaine, *Drug Dev. Ind. Pharm.* 23 (1997) 1159–1165. doi:10.3109/03639049709146153.
- [7] C. Guo, J. Wang, F. Cao, R.J. Lee, G. Zhai, Lyotropic liquid crystal systems in drug delivery, *Drug Discov. Today.* 15 (2010) 1032–1040. doi:10.1016/j.drudis.2010.09.006.
- [8] M. Makai, E. Csanyi, Z. Nemeth, J. Palinkas, I. Eros, Structure and drug release of lamellar liquid crystals containing glycerol, *Int J Pharm.* 256 (2003) 95–107. <http://www.ncbi.nlm.nih.gov/pubmed/12695015>.
- [9] C.C. Muellergoymann, S.G. Frank, Interaction of Lidocaine and Lidocaine-Hcl with the Liquid-Crystal Structure of Topical Preparations, *Int J Pharm.* 29 (1986) 147–159. doi:10.1016/0378-5173(86)90112-2.
- [10] H.S. Amelia Yip Anna Taddio, Review of a New Topical Anesthetic, Liposomal Lidocaine, for Procedural Pain in Children, *Can. J. Hosp. Pharm.* 58 (2005) 148–150.
- [11] R.H. Muller, M. Radtke, S.A. Wissing, Solid lipid nanoparticles (SLN) and nanostructured lipid carriers (NLC) in cosmetic and dermatological preparations, *Adv Drug Deliv Rev.* 54 Suppl 1 (2002) S131–55. <http://www.ncbi.nlm.nih.gov/pubmed/12460720>.
- [12] S. Kuchler, W. Herrmann, G. Panek-Minkin, T. Blaschke, C. Zoschke, K.D. Kramer, R. Bittl, M. Schafer-Korting, SLN for topical application in skin diseases--characterization of drug-carrier and carrier-target interactions, *Int J Pharm.* 390 (2010) 225–233. doi:10.1016/j.ijpharm.2010.02.004.
- [13] S. Doktorovova, E.B. Souto, Nanostructured lipid carrier-based hydrogel formulations for drug delivery: a comprehensive review., *Expert Opin. Drug Deliv.* 6 (2009) 165–176. doi:10.1517/17425240802712590.
- [14] C.H. Loo, M. Basri, R. Ismail, H.L.N. Lau, B.A. Tejo, M.S. Kanthimathi, H.A. Hassan, Y.M. Choo, Effect of compositions in nanostructured lipid carriers (NLC) on skin hydration and occlusion, *Int. J. Nanomedicine.* 8 (2013) 13–22. doi:10.2147/IJN.S35648.
- [15] P. Desai, R.R. Patlolla, M. Singh, Interaction of nanoparticles and cell-penetrating peptides with skin for transdermal drug delivery, *Mol Membr Biol.* 27 (2010) 247–259. doi:10.3109/09687688.2010.522203.
- [16] S.A. Wissing, R.H. Muller, The influence of solid lipid nanoparticles on skin hydration and viscoelasticity--in vivo study, *Eur J Pharm Biopharm.* 56 (2003) 67–72. <http://www.ncbi.nlm.nih.gov/pubmed/12837483>.
- [17] C. Puglia, P. Blasi, L. Rizza, A. Schoubben, F. Bonina, C. Rossi, M. Ricci, Lipid nanoparticles for prolonged topical delivery: an in vitro and in vivo investigation, *Int J Pharm.* 357 (2008) 295–304. doi:10.1016/j.ijpharm.2008.01.045.
- [18] M. Ricci, C. Puglia, F. Bonina, C. Di Giovanni, S. Giovagnoli, C. Rossi, Evaluation of indomethacin percutaneous absorption from nanostructured lipid carriers (NLC): in vitro and in vivo studies, *J Pharm Sci.* 94 (2005) 1149–1159. doi:10.1002/jps.20335.
- [19] F. Castelli, C. Puglia, M.G. Sarpietro, L. Rizza, F. Bonina, Characterization of indomethacin-loaded lipid nanoparticles by differential scanning calorimetry, *Int J Pharm.* 304 (2005) 231–238. doi:10.1016/j.ijpharm.2005.08.011.
- [20] C. Puglia, R. Filosa, A. Peduto, P. de Caprariis, L. Rizza, F. Bonina, P. Blasi, Evaluation of alternative strategies to optimize ketorolac transdermal delivery, *AAPS PharmSciTech.* 7 (2006) 64. doi:10.1208/pt070364.
- [21] K. Bhise, S.K. Kashaw, S. Sau, A.K. Iyer, Nanostructured lipid carriers employing polyphenols as promising anticancer agents: Quality by design (QbD) approach, *Int J Pharm.* 526 (2017) 506–515. doi:10.1016/j.ijpharm.2017.04.078.
- [22] J.C. Visser, W.M. Dohmen, W.L. Hinrichs, J. Breitzkreutz, H.W. Frijlink, H.J. Woerdenbag, Quality by design approach for optimizing the formulation and physical properties of extemporaneously prepared orodispersible films, *Int J Pharm.* 485 (2015) 70–76. doi:10.1016/j.ijpharm.2015.03.005.
- [23] ICH Q8, ICH Guideline Pharmaceutical Development Q8(R2), (2009).
- [24] E. Pallagi, R. Ambrus, P. Szabo-Revesz, I. Csoka, Adaptation of the quality by design concept in early

- pharmaceutical development of an intranasal nanosized formulation, *Int J Pharm.* 491 (2015) 384–392. doi:10.1016/j.ijpharm.2015.06.018.
- [25] A. Kovacs, S. Berko, E. Csanyi, I. Csoka, Development of nanostructured lipid carriers containing salicylic acid for dermal use based on the Quality by Design method, *Eur J Pharm Sci.* 99 (2017) 246–257. doi:10.1016/j.ejps.2016.12.020.
- [26] B. Shah, D. Khunt, H. Bhatt, M. Misra, H. Padh, Intranasal delivery of venlafaxine loaded nanostructured lipid carrier: Risk assessment and QbD based optimization, *J. Drug Deliv. Sci. Technol.* 33 (2016) 37–50. doi:10.1016/j.jddst.2016.03.008.
- [27] H. Raina, S. Kaur, A.B. Jindal, Development of efavirenz loaded solid lipid nanoparticles: Risk assessment, quality-by-design (QbD) based optimisation and physicochemical characterisation, *J. Drug Deliv. Sci. Technol.* 39 (2017) 180–191. doi:10.1016/j.jddst.2017.02.013.
- [28] ICH Q9, Quality Risk Management Guidance for Industry Dated June, (2006). available from: [www.fda.gov/downloads/Drugs/.../Guidances/ucm073511.pdf](http://www.fda.gov/downloads/Drugs/.../Guidances/ucm073511.pdf).
- [29] N.A. Charoo, A.A. Shamsher, A.S. Zidan, Z. Rahman, Quality by design approach for formulation development: a case study of dispersible tablets, *Int J Pharm.* 423 (2012) 167–178. doi:10.1016/j.ijpharm.2011.12.024.
- [30] R. Thatipamula, C. Palem, R. Gannu, S. Mudragada, M. Yamsani, Formulation and in vitro characterization of domperidone loaded solid lipid nanoparticles and nanostructured lipid carriers, *Daru.* 19 (2011) 23–32. <http://www.ncbi.nlm.nih.gov/pubmed/22615636>.
- [31] A.M. Kligman, E. Christophers, Preparation of Isolated Sheets of Human Stratum Corneum, *Arch Dermatol.* 88 (1963) 702–705. <http://www.ncbi.nlm.nih.gov/pubmed/14071437>.
- [32] I. Dierking, *Textures of liquid crystals*, Wiley-VCH, Weinheim, 2003.
- [33] L. Voelker-Pop, Optical methods in rheology: Polarized light imaging, *Chem. List.* 108 (2014) 707–710.
- [34] J. Zhang, Y. Fan, E. Smith, Experimental design for the optimization of lipid nanoparticles, *J Pharm Sci.* 98 (2009) 1813–1819. doi:10.1002/jps.21549.
- [35] N. Anton, J.P. Benoit, P. Saulnier, Design and production of nanoparticles formulated from nano-emulsion templates-a review, *J Control Release.* 128 (2008) 185–199. doi:10.1016/j.jconrel.2008.02.007.
- [36] H.M. Badawi, W. Forner, S.A. Ali, The conformational stability, solvation and the assignments of the experimental infrared, Raman, (1)H and (13)C NMR spectra of the local anesthetic drug lidocaine, *Spectrochim Acta A Mol Biomol Spectrosc.* 142 (2015) 382–391. doi:10.1016/j.saa.2015.02.005.
- [37] L.B. Jensen, K. Petersson, H.M. Nielsen, In vitro penetration properties of solid lipid nanoparticles in intact and barrier-impaired skin, *Eur J Pharm Biopharm.* 79 (2011) 68–75. doi:10.1016/j.ejpb.2011.05.012.
- [38] P. You, R. Yuan, C. Chen, Design and evaluation of lidocaine- and prilocaine-co-loaded nanoparticulate drug delivery systems for topical anesthetic analgesic therapy: A comparison between solid lipid nanoparticles and nanostructured lipid carriers, *Drug Des. Devel. Ther.* 11 (2017) 2743–2752. doi:10.2147/DDDT.S141031.
- [39] M. Franz-Montan, D. Baroni, G. Brunetto, V.R.V. Sobral, C.M.G. da Silva, P. Venâncio, P.W. Zago, C.M.S. Cereda, M.C. Volpato, D.R. de Araújo, E. de Paula, F.C. Groppo, Liposomal lidocaine gel for topical use at the oral mucosa: characterization, in vitro assays and in vivo anesthetic efficacy in humans., *J. Liposome Res.* 25 (2014) 11–19. doi:10.3109/08982104.2014.911315.
- [40] S. Babaei, S. Ghanbarzadeh, Z.M. Adib, M. Kouhsoltani, S. Davaran, H. Hamishehkar, Enhanced skin penetration of lidocaine through encapsulation into nanoethosomes and nanostructured lipid carriers: A comparative study, *Pharmazie.* 71 (2016) 247–251. doi:10.1691/ph.2016.5158.
- [41] L. H., Oleogels – what non-aqueous products can accomplish, *Kosmet. Prax.* 4 (2004).
- [42] S.H. Moghadam, E. Saliq, S.D. Wettig, C. Dong, M. V. Ivanova, J.T. Huzil, M. Foldvari, Effect of chemical permeation enhancers on stratum corneum barrier lipid organizational structure and interferon alpha permeability, *Mol. Pharm.* 10 (2013) 2248–2260. doi:10.1021/mp300441c.
- [43] S. Wissing, A. Lippacher, R. Muller, Investigations on the occlusive properties of solid lipid nanoparticles (SLN), *J Cosmet Sci.* 52 (2001) 313–324. <http://www.ncbi.nlm.nih.gov/pubmed/11567210>.
- [44] M. Foldvari, Non-invasive administration of drugs through the skin: challenges in delivery system design, *Pharm Sci Technol Today.* 3 (2000) 417–425. <http://www.ncbi.nlm.nih.gov/pubmed/11116201>.
- [45] H. Iwai, J. Fukasawa, T. Suzuki, A liquid crystal application in skin care cosmetics, *Int J Cosmet Sci.* 20 (1998) 87–102. doi:10.1046/j.1467-2494.1998.171741.x.